

See discussions, stats, and author profiles for this publication at: <https://www.researchgate.net/publication/7000250>

Electron transfer processes on Ag and Au clusters supported on TiO₂(110) and cluster size effects

ARTICLE *in* THE JOURNAL OF CHEMICAL PHYSICS · JUNE 2006

Impact Factor: 2.95 · DOI: 10.1063/1.2205849 · Source: PubMed

CITATIONS

16

READS

12

2 AUTHORS, INCLUDING:



Vladimir Esaulov

French National Centre for Scientific Research

206 PUBLICATIONS 1,843 CITATIONS

SEE PROFILE

Electron transfer processes on Ag and Au clusters supported on TiO₂(110) and cluster size effects

Ana Rita Canário

Laboratoire des Collisions Atomiques et Moléculaires (Unité Mixte CNRS Université UMR8625), bât 351, Université Paris Sud, 91405 Orsay, France and CEFIC, Departamento de Física, Universidade de Lisboa, 2829-516 Caparica, Portugal

Vladimir A. Esaulov^{a)}

Laboratoire des Collisions Atomiques et Moléculaires (Unité Mixte CNRS Université UMR8625), bât 351, Université Paris Sud, 91405 Orsay, France

(Received 22 November 2005; accepted 20 April 2006; published online 13 June 2006)

The results of a detailed study of Li⁺ neutralization in scattering on Ag and Au clusters and thin films supported on TiO₂ are presented. A very efficient neutralization is observed on small clusters with a decrease for the smallest clusters. These results closely follow the size-effects observed in the reactivity of these systems. The energy dependence of the neutralization was studied for the larger clusters (>4 nm) and observed to be similar in trend to the one observed on films and bulk (111) crystals. A general discussion of possible reasons of the enhancement in neutralization is presented and these changes are then tentatively discussed in terms of progressive modifications in the electronic structure of clusters as a function of reduction in size and as it evolves from metallic-like to discretised states. The highest neutralization efficiency would appear to correspond to clusters sizes for which a metal to nonmetal transition occurs. The relative position of the Li level and the highest occupied molecular orbital in the molecular cluster can be expected to strongly affect the electron transfer processes, which in this case should be described in a molecular framework.

© 2006 American Institute of Physics. [DOI: [10.1063/1.2205849](https://doi.org/10.1063/1.2205849)]

I. INTRODUCTION

Supported metal nanoparticles have attracted much attention because of their use in many fields such as heterogeneous catalysis, microelectronics, photonics, etc. It is a well established fact that the size, shape, and nature of the support, affect the properties of the nanoparticles and can play a crucial role in determining their use in a particular application. A considerable effort is being made to understand the various aspects that govern the properties of these systems, although a full understanding has not been achieved.^{1–7} The size effects have been discussed in terms of morphology and electronic structure and questions of the interaction with the substrate are addressed.

The electronic structure and shape of the metal clusters are to a certain extent related. As a function of increasing size, the electronic structure of the clusters evolves from the extreme case of the atomic structure of its constituent atoms, to the formation of a system with molecular character, which progressively evolves to that of a band structure of the bulk metal. The molecular aggregate is characterized by an energy gap between occupied and unoccupied levels. The increase in size of the system progressively leads to the disappearance of this gap and transition towards the valence band structure of the metal. According to existing literature the number of atoms that are necessary to induce this transition may range from several tens to several hundred (see e.g., Refs. 2 and

6–11). These evolutions have been recently studied in a series of elegant scanning tunnel microscopy (STM) studies for various metal clusters on various substrates.^{10–15} An interesting question that has been recently addressed regards the electronic structure of the “metallic” clusters and two- and three-dimensional quantum confinement effects.^{10–12}

In general the surface science studies performed concern the growth of metallic clusters, their morphology, electronic structure, photonic response, and magnetic properties and reactivity involving reactions with various gasses in relation with catalysis problems and selectivity. In gas surface reactions electron transfer processes involving electrons near the Fermi level are very important. This is also the case for resonant neutralization of some positive ions and negative ion formation. In ion/atom/molecule-surface interactions these have been studied quite extensively using scattering techniques that allow one to obtain detailed information of the dynamics of these processes.^{16–19} These studies have provided a wealth of data for theoretical modeling, which is inaccessible in “static” studies regarding only adsorption or study of the nature of reaction products. Electron transfer processes in ion/atom-surface interactions are very sensitive to the electronic structure of both partners and could be used as a probe of the surface electronic structure²⁰ and such studies for the case of supported clusters appear interesting. Until recently the case of supported metal clusters has, however, not been addressed and in this paper we describe our first detailed study of electron transfer on the example of Li⁺ ion resonant neutralization on Ag and Au clusters supported on

^{a)} Author to whom correspondence should be addressed. Electronic mail: esaulov@lcam.u-psud.fr

rutile $\text{TiO}_2(110)$. Very recently a brief account of a similar study of 2 keV Na^+ neutralization on Au clusters on TiO_2 was published by Liu *et al.*²¹ who found that the neutralization was much more probable on small clusters than on bulk gold samples and suggest that this may be used in “detection of quantum confined states.”

Our choice of these systems was dictated largely by the fact that the Ag/Au cluster growth has also been recently extensively studied and these studies form a basis for our investigation. Some aspects are briefly outlined below.

Particular attention has been paid to Au/ TiO_2 since the discovery made by Haruta *et al.*²² that nanosized, supported gold clusters exhibit unique catalytic properties. Gold is normally quite inert, but in the form of nanoclusters on a metal oxide, it can oxidize CO at remarkably low temperatures.^{22–24} Besides low-temperature CO oxidation, nanosized Au clusters supported on oxides are active for a number of other industrially important catalytic reactions such as, e.g., NO reduction, hydrogenation, water gas-shift reaction, and partial oxidation of hydrocarbons.²⁵ Similarly, small Ag clusters on metal oxide supports have proved to be active in a number of reactions. They promote selective oxidation of ethylene to ethylene oxide²⁶ and methanol to formaldehyde.²⁷ Oliveira *et al.*²⁸ have shown that TiO_2 supported small Ag catalysts (cluster sizes from 2 to 4 nm) are also active for low-temperature CO oxidation and propylene epoxidation, indicating that the properties exhibited by supported nano Au particles are not unique.

In the case of CO reduction, Valden *et al.*¹³ and Haruta *et al.*²² reported a strong size effect, Au particles above 5 nm exhibit virtually no activity while particles below 5 nm show good activity for room temperature CO oxidation. Valden *et al.*¹³ and Bamwenda *et al.*²⁹ have observed a strong particle size effect with particles in the 2.5–3.5 nm range showing a maximum in activity. Goodman and co-workers^{13,30} performed a series of scanning tunnelling spectroscopy (STS), and CO oxidation kinetics studies of Au vapor-deposited onto a $\text{TiO}_2(110)$ single crystal and a TiO_2 thin film. Maximum catalytic activity for these clusters was found to coincide with the metal-to-nonmetal transition occurring in clusters with a diameter of approximately 3.0 nm, as determined by STS cluster band gap measurements. This cluster diameter also coincides with a cluster growth transition from the nucleation of flat, two-dimensional clusters, to their agglomeration into hemispherical, three-dimensional structures, as measured by STM. A summary of the present level of understanding of the Au-catalyzed CO oxidation reaction has been recently presented by Diebold,³¹ indicating that in spite of the numerous studies available, a controversy still exists concerning the question whether there is a dominant factor or if several effects simultaneously contribute to the special catalytic properties of the supported nanosized gold particles.

In this paper, we will describe the results of our investigation of Li^+ neutralization on Ag and Au clusters vapor deposited in ultrahigh vacuum (UHV) at room temperature on $\text{TiO}_2(110)$. As a prelude to this paper, we previously reported on our study of the growth of Ag clusters on $\text{TiO}_2(110)$ for different evaporation fluxes in which we observed formation of various size clusters with average cluster

size distributions ranging from large clusters of 20 nm to small clusters of less than 5 nm (this size limitation was given by the scanning electron microscope resolution of 3 nm).³² Formation of Ag clusters of smaller sizes was investigated by, e.g., Goodman and co-workers.^{33,34}

We shall present a study of neutralization as a function of cluster sizes and a Li ion energy range from a few hundred eV to 1.5 keV. This was supplemented by the study of neutralization on Ag and Au films and extended to the case of polycrystalline Ag, Ag(100) (Ref. 35) and finally Ag(111), Au(111), and Cu(111) surfaces, which will be mentioned in the discussion, but is the object of a separate publication.³⁶ Li^+ neutralization on simple metal surfaces describable within a jellium model of resonant tunnelling is now quite well understood.^{35,37} The description of resonant charge transfer for the case of metal surfaces exhibiting specific band gaps and surface states is still problematic however, though in some cases quite good agreement between experiment and theory within a wave packet propagation approach³⁸ has been recently achieved.^{35,39–41}

II. EXPERIMENT

The experiments are performed in an UHV system.³² The system is equipped with a low-energy electron diffraction (LEED)/Auger system, a differentially pumped ion gun used for low-energy ion scattering (LEIS) and Ar sputtering, and a Li ion gun which uses a getter source. LEIS measurements were performed using a tandem (dual) parallel plate electrostatic analyzer. Time of flight measurements were made using a tube, equipped with a channel plate detector set behind the electrostatic analyzers allowing energy loss investigation of scattered ions and neutrals with a total flight length of 116 cm. This ensemble (analyzer and time-of-flight (TOF) tube) is located at 120° with respect to the He/Ar ion source. The Li gun is located at an angle of 114° from the analyzer/TOF system and is “out of scattering plane” with respect to the sputter-gun-analyzer by 45° .

Our measurements on neutralization probabilities involve low Li^+ beam flux, pulsed beam time of flight measurements. This precludes ion implantation effects. This was, however, regularly checked by performing the same type of measurement (e.g., at a given energy, or a given coverage) in different conditions, i.e., in the beginning or end of a series of measurements or for different coverage “steps.” We thus exclude that our results are affected by Li implantation.

The polished $\text{TiO}_2(110)$ single crystal is a 1 mm thick $10 \times 10 \text{ mm}^2$. The sample is attached to a Ta plate, and mounted on a XYZ rotary manipulator. The sample is heated through a combination of radiation and electron bombardment using a tungsten filament positioned behind it. The sample is partially reduced by annealing at about 900 K in a UHV chamber. After this treatment, the bulk becomes an *n*-type semiconductor and this eliminates any charging problems in Auger electron spectroscopy (AES) and LEIS measurements—an important point in this work. The sample, which is initially transparent, becomes dark blue after extensive reduction. Our usual sample preparation included cycles of 1 keV Ar sputtering at 10° – 20° incidence with respect to

the surface plane and 10 min annealing at 900 K as measured on the Ta plate. The clean surface presents a sharp LEED pattern corresponding to 1×1 structure.

The chamber is equipped with a dual cell, cooled, movable metal evaporation source, and a quartz crystal microbalance (QCM). The QCM is located above the sample at the same distance from the evaporator as the sample and can be put in front of the evaporator by vertical translation ensuring that the evaporation rate measured on the QCM is the same as on the sample. In the present study Ag and Au evaporation was performed by wrapping a thin wire around a heated tungsten filament. The temperature of the W filament was determined by a thermocouple wound around the tungsten wire along with the Ag or Au wire.

The evaporation was performed after the TiO₂ crystal had cooled down to room temperature. The deposition rate was generally varied between 0.002 and 0.7 eq mL (where 1 eq mL = 1 monolayer; corresponds to 1.4×10^{15} atom/cm²). During evaporation, the pressure in the chamber increases to about 4.6×10^{-10} mbar. The QCM is used to evaluate the evaporation rate and indicate the average amount of deposited silver (eq ML). Evaporation was performed after stabilization of the source conditions, i.e., tungsten filament current, temperature, and evaporation rate.

As described previously, growth was monitored *in situ* mainly by LEIS using He⁺ and Li⁺ ion scatterings. The He⁺ LEIS monitoring was performed at variable intervals of times to exclude sputtering effects (see comments in Ref. 32). During the He⁺ LEIS and the TOF Li⁺ measurements the crystal was turned away from the evaporator and the evaporation was briefly stopped for the measurement time of a few minutes (typically 5–10 min depending upon Li ion energies and count rates). In this study we rely mainly on our previously described study of Ag growth on TiO₂ (Ref. 32) and the study of Goodman and co-workers on both Ag and Au clusters.^{33,34}

A point that should be noted is that in different similar series of measurements, even though the surface preparation conditions and evaporation flux may be the same, in the absence of *in situ* STM measurements we cannot be sure that the cluster size distributions are quite the same. Thus although the general trends of the measurements and the magnitude of the neutralization probabilities are the same, the same effective coverage determined on the basis of QCM flux measurement and exposure time may not correspond exactly to the same size distribution. Here we therefore present some typical series of measurements, without averaging over different series.

III. RESULTS

A. Li⁺ neutralization on Ag clusters on TiO₂(110)

This section presents the results obtained on the neutralization of Li⁺ ions on Ag clusters supported on TiO₂(110). As mentioned above, in our previous work³² we observed that the cluster sizes depended on evaporation rates. At very low rates we observed the formation of large sized distantly placed clusters, that attained an average size of up to 20 nm “diameter” for an evaporation rate of 0.002 eq ML/min. For

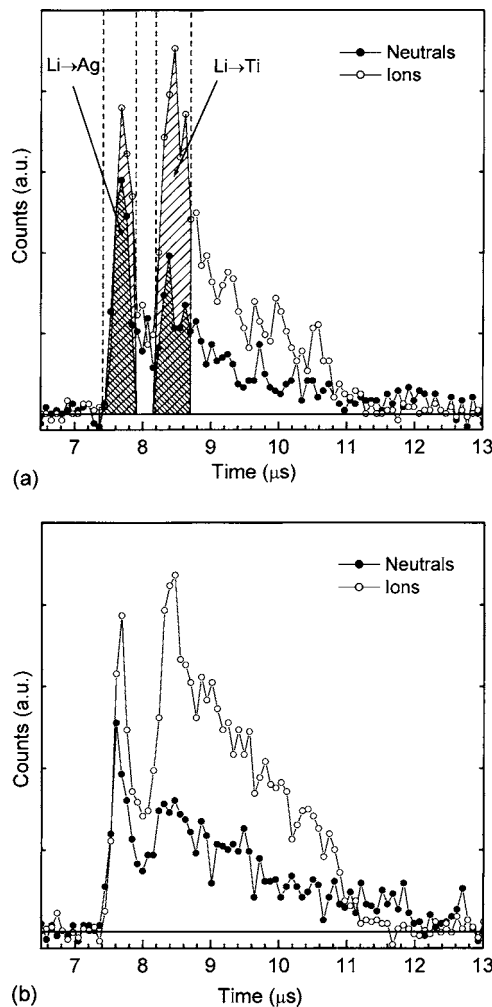


FIG. 1. Li⁺ TOF spectra (1 keV) on TiO₂ with 1 eq ML of Ag deposited at 0.08 eq ML/min for two different scattering conditions: (a) exit normal to the surface and (b) close to specular conditions (exit angle 60°).

“intermediate” rates of the order of 0.02 eq ML/min we observed cluster sizes of the order of 10 nm. For “high” rates of the order of 0.1 eq ML/min we observed small clusters of less than 5 nm (this size limitation was given by the scanning electron microscope resolution of 3 nm). The latter concurs with the work of Lai *et al.*³³ where similar evaporation rates were used and cluster sizes of the order of 2–3 nm have been observed. As a function of Ag deposition one can expect some evolution of cluster size. In our earlier study, SEM measurements were performed *ex situ* after deposition and hence this evolution could not be monitored. Here we measured the neutralization fraction as a function of coverage and for different evaporation rates. It was thought that for the higher evaporation rates we would be able to follow transition from very small clusters (<1 nm) to clusters of the order of 5 nm. At the very low rates it seemed that it could be possible to observe the evolution from two-dimensional (2D) to three-dimensional (3D) growth for the large clusters. Note that in the rest of this section we will refer to small, medium, and large clusters, where in accordance with this paragraph we imply clusters of mean diameter sizes of about 5, 10, and 20 nm.

Figure 1 presents typical time of flight spectra for ions

and neutrals obtained with 1 keV Li^+ ions on $\text{TiO}_2(110)$ substrate where 1 eq ML of Ag was deposited at rate of 0.08 eq ML/min. In the time of flight spectra of the backscattered Li^+ ions and neutrals two well defined peaks can be observed, assignable to scattering on surface Ag and Ti atoms, respectively. For a reader unfamiliar with ion scattering techniques, we note that the final energy of the backscattered Li projectile can be estimated simply from classical mechanics considering scattering of Li mass M_1 off a target atom of mass M_2 , through the 114° scattering angle. For 1 keV Li ions the final energy of backscattered Li ions/atoms is of 835 eV for single scattering conditions. For other energies a similar multiplying factor applies. There is also a “background” component, due to multiple scattering events but the two “surface” peaks are clearly identifiable. The spectra for backscattered ions and neutrals are very similar.

From these TOF spectra, we extract the neutralization probability for Li ions which experienced binary collisions with surface atoms. This probability (P_{Ag} or P_{Ti}) is calculated using the integrated area in the hatched zones depicted in Fig. 1(a) for each peak and is defined by $P_{\text{Ag}} = f(\text{Ag}_{\text{neutral}})/(f(\text{Ag}_{\text{neutral}}) + f(\text{Ag}_{\text{ions}}))$

One has to be careful when calculating the probability for neutralization for Ti since the Ti surface peak has a contribution from Li ions that undergo multiple collisions and this contribution also increases with increasing Ag coverage. Therefore, in such cases, correct evaluation of Ti should be preceded by the subtraction of this background component. In this paper we do not focus on neutralization on Ti. For the spectra shown in Fig. 1(a) the neutral fraction obtained is $(46\% \pm 2\%)$ and $(27\% \pm 2\%)$ on Ag and Ti atoms, respectively.

Measurements were made for different incidence angles. In Fig. 1 we show two situations corresponding to almost specular scattering (exit angle of 60°) and an exit normal to the surface. The neutral fraction is found to be somewhat higher in the first case. The difference is not very large (41% in the “specular case”). It should be noted that it is somewhat difficult to assign in general exactly the angle with respect to the cluster surface. This is straightforward for 2D clusters or even clusters with large flat terraces. According to Goodman and co-workers^{33,34} the 3D clusters are hemispherical. Optical, plasmon shift measurements of Martin *et al.* suggest a spheroidal shape.⁴² In this case angle assignment becomes difficult. Given that in normal exit conditions the interaction with the topmost surface atoms is enhanced compared to specular scattering conditions, subsequent data is given for ions *exiting* normal to the sample surface plane.

Figures 2(a) and 2(b) present the neutralization fraction on the Ag clusters as a function of coverage for two different final coverages, using the indicated evaporation rates. In each case, the insets (i), (ii), and (iii) show the ion and neutral spectra at the indicated Ag coverage. As in Fig. 1 the peak for flight times above $8 \mu\text{s}$ corresponds to scattering off Ti, while the one below $8 \mu\text{s}$ to scattering off Ag. For small Ag coverages the Ag peak is small, while for large Ag coverages the Ti peak essentially disappears, indicating an essentially Ag covered surface. The error bar in the neutraliza-

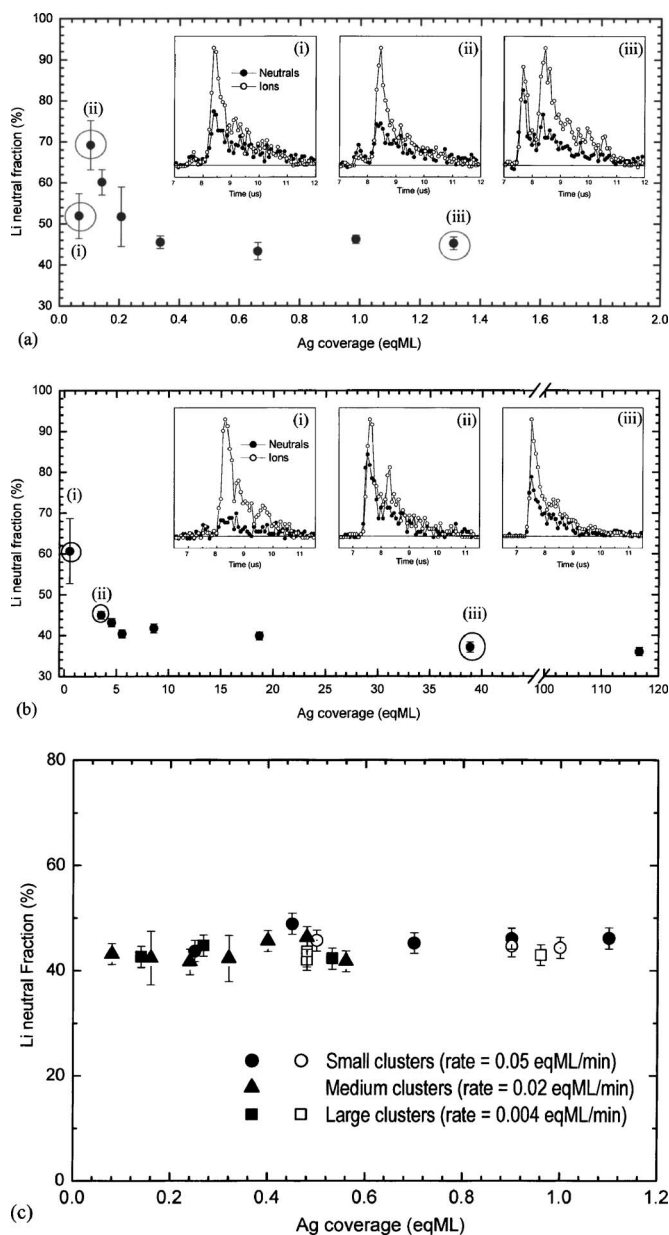


FIG. 2. Li neutral fraction dependence on Ag coverage for small clusters deposited at a rate of 0.08 eq ML/min (a) and 1 eq ML/min (b). In each case the insets (i), (ii), and (iii) show the TOF spectra for neutrals and ions at the indicated coverage. (c) Li neutral fraction dependence on Ag coverage for different cluster sizes.

tion fraction is calculated for each pair of spectra and depends on the signal to noise ratio close to the Ag surface peak.

For small coverages a higher neutral fraction is obtained than at larger coverages. In fact, the Li neutral fraction tends rapidly to a saturation value below 40%. An interesting feature is that a *smaller* value of the neutral fraction is also obtained at the very beginning of the deposition [Fig. 2(a)], i.e., for the smallest clusters.

Results of additional measurements made using other evaporation rates are summarized in Fig. 2(c). In all these measurements the neutral fraction was found to have attained its final value of about 42% and no dependence on coverage was obtained, which could be attributable to a transition from 2D to 3D structures.

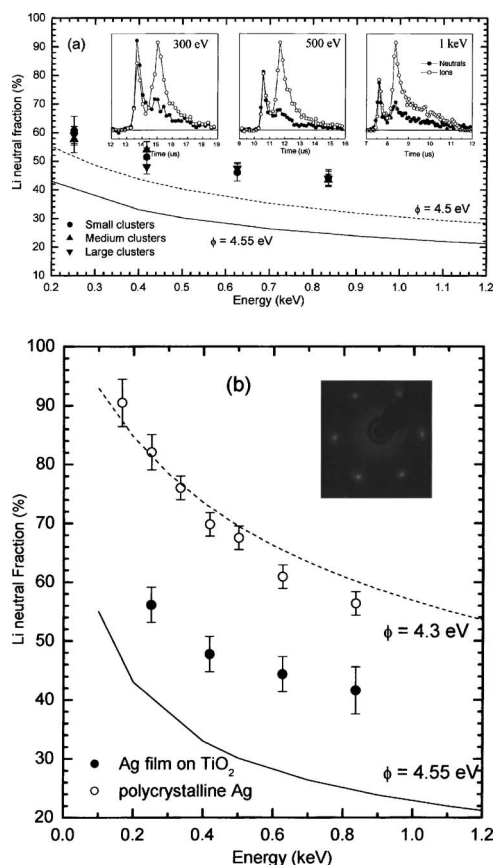


FIG. 3. (a) Exit energy dependence of the Li neutral fraction for different Ag cluster sizes. The insets show the TOF spectra for some incident energies. (b) Energy dependence of the Li neutral fraction for a Ag film on TiO₂ (LEED pattern obtained after the deposition shown in the inset) and a bulk polycrystalline Ag sample. In both cases, the continuous lines show the calculated neutral fraction with a jellium model of a surface with the specified work function.

As discussed previously by us on the example of Li⁺ neutralization on Ag(100) single crystal,³⁵ the energy dependence of the neutral fraction contains essential information on the dynamics of the charge transfer processes. The energy dependence of the Li neutral fraction for different Ag cluster sizes is shown in Fig. 3(a), as a function of the exit energy of the projectile. For each incident energy of the projectile, TOF spectra of the backscattered neutrals and ions were acquired and the neutral fraction on the Ag surface peak was calculated. The insets of Fig. 3(a) show typical ion and neutral TOF spectra for incident ions with energies of 0.3, 0.5, and 1 keV, respectively. The energy dependence for the small, medium and large clusters was measured at the end of each deposition series. Note that in the case of Fig. 2(a) this would have corresponded to the spectrum labeled as (iii). The neutralization probability for 1 keV incident Li ions (with exit energy of 835 eV) is always close to 42% irrespectively of the mean cluster size.

We attempted to measure the energy dependence for the extremely small clusters, where the neutralization fraction was higher than 50% at 1 keV, but the feeble intensity makes these measurements very difficult to accomplish with sufficiently high accuracy and we do not report them here. One of the problems here is related to sputtering effects, which have to be minimized for meaningful measurements.

From analysis of Fig. 3, we conclude that the energy dependence of the neutralization probability does not present any significant variation with the mean Ag cluster size for sizes larger than about 3 nm. In Fig. 3 we also show a calculation of the neutralization probability for work function values of 4.5 and 4.55 eV. In this calculation we use rates calculated within the jellium model³⁵ and assume that a Li⁺ ion leaves normal to the surface and that neutralization occurs in the outgoing path with the exit (final) velocity of the Li ion. As may be seen our results follow the same general trend.

In order to obtain a clearer view of the results for the larger clusters and the higher coverages, a thick Ag film was deposited on the TiO₂(110) surface. To achieve the substrate's metallization, a high deposition rate was used (about 1 eq ML/min) and complete coverage of the surface was obtained. This was verified by He⁺ scattering, where only the Ag peak was visible, and by Li scattering, as the Ti surface peak ceased to be visible both in the neutral and in the ion TOF spectra. At last, a visual inspection of the final surface showed a clear metallic round spot.

The Li⁺ neutralization probability measured for this thick Ag film is shown in Fig. 3(b), and compared with similar results for a polycrystalline bulk Ag sample, which we also studied. Also shown are the calculated neutral fractions for jellium surface with work function of 4.3 and 4.55 eV.

The work function of polycrystalline Ag is 4.3 eV,⁴³ and the experimental results follow closely the expected dependence for a jellium surface with this work function. In the case of the complete coverage of the TiO₂ surface, the neutral fraction of the Ag film is significantly lower than the one obtained for polycrystalline Ag. A LEED pattern was obtained for the deposited film and indicated the formation of a well ordered close packed Ag(111) surface as shown in the inset in Fig. 3(b). The work function of Ag(111) is about 4.55 eV.⁴³ Our results for the film and the clusters appear to be somewhat higher. This effect could be related to the existence of the Ag(111) surface *L* gap and eventual role played by the surface states (see discussion in our paper on Ag(100)). We shall return to this point below and in a separate publication,³⁶ where measurements for fcc (111) noble metal surfaces are discussed. We note here that results for the Ag(111) crystal³⁶ yield values similar to those for the film.

B. Li⁺ neutralization on Au clusters on TiO₂(110)

The system Au/TiO₂ has been thoroughly investigated by several groups (see, e.g., Refs. 15 and 44–47). Lai *et al.*¹⁵ indicate that with increasing Au coverage, the cluster size increases continuously, while the increase in cluster density is limited. Below 0.1 eq ML Au, the mean diameter of the clusters is less than 2 nm, with height of 1 or 2 atomic layers (quasi-2D clusters). Increasing the deposition amount from 0.1 to 2.0 eq ML increases the cluster size from 2 to 5 nm mean diameter (3D growth). The influence of flux on the morphology of the supported Au clusters was not investigated by these authors. The deposition rate used by these authors was about 0.1 eq ML/min and we used this rate.

Figure 4(a) presents typical time of flight spectra ob-

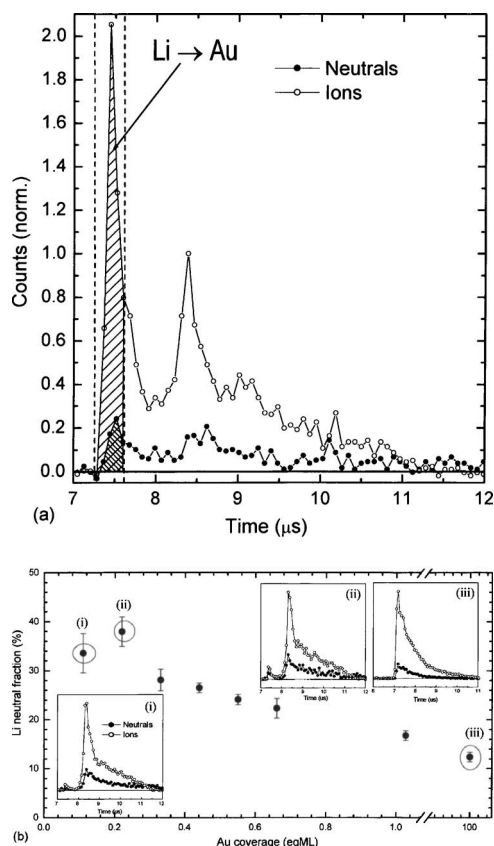


FIG. 4. (a) Li^+ TOF spectra (1 keV incident ions) on TiO_2 with 1 eq ML of Au deposited at 0.1 eq ML/min as a function of time. (b) Li neutral fraction dependence on Au clusters supported on TiO_2 (deposition rate ≈ 0.1 eq ML/min). The insets (i), (ii), and (iii) show the TOF spectra for neutrals and ions at the indicated coverage.

tained with 1 keV Li^+ ions on $\text{TiO}_2(110)$ substrate where 1 eq ML Au was deposited at 0.1 eq ML/min. In the time of flight spectra of the backscattered Li^+ ions and neutrals we observe two well defined peaks assignable to scattering on surface Au (below 8 μs) and Ti (above 8 μs) atoms, respectively. The background component is visible, but the overlap between the Au and Ti surface peaks is smaller than in the Ag/ TiO_2 case. This is due to the lower energy loss for the Li ions in binary collision with Au atoms than with Ag atoms. As in the case of silver clusters, the spectra for backscattered ions and neutrals are very similar.

Figure 4(b) displays the results of the Li^+ 1 keV neutralization fraction on the Au clusters versus coverage. The Li^+ neutralization probability clearly decreases with increasing cluster size, attaining a value of around 10%–15% for larger clusters. For smaller clusters, with mean diameter of less than 3 nm (relating our conditions to those of Ref. 15) a neutral fraction of 35% is obtained.

Thus the Li neutralization on gold clusters occurs more efficiently on the small clusters attaining values almost four times higher than on Au film in the asymptotic limit (see below). As for the case of Ag (Fig. 3), from the data in Fig. 4, it appears that for the smallest cluster size there may be decrease in the neutralization. Our results on Li neutralization on Au clusters are thus qualitatively similar to those of Liu *et al.*,²¹ who observed a larger neutralization probability for Na neutralization on Au clusters for small cluster sizes.

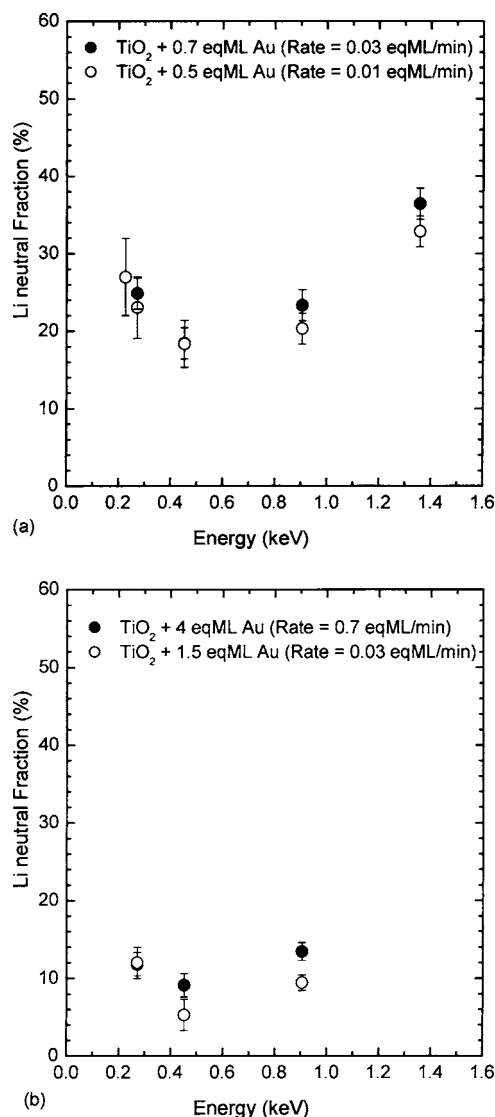


FIG. 5. Energy dependence of the Li neutral fraction for Au clusters on TiO_2 for small Au clusters (a), and large Au clusters (b). The small clusters are expected to have a mean diameter of approximately 4.5 nm and the larger ones of at least 6 nm, according to Lai *et al.* (Ref. 15). The inset (i) shows the original spectra at the indicated coverage.

The energy dependence of the Li neutral fraction for different Au cluster sizes is shown in Fig. 5, as function of the exit energy of the projectile. For each incident energy of the projectile, TOF spectra of the backscattered neutrals and ions were acquired and the neutral fraction on the Au surface peak was calculated. The dependence of the neutral fraction on the projectile's energy is drastically different from the one found for the Ag clusters. For exit energies up to 300 eV, the neutral fraction *slowly* decreases with increasing energy, whereas for higher energies it exhibits a continuous growth. The energy dependence was investigated for different cluster sizes (different coverages). In Fig. 5(a), measurements for Au clusters with a neutralization probability around 20% (for 1 keV incident Li^+ ions) are shown. These clusters are expected to have a mean diameter of approximately 4 nm, according to Lai *et al.*¹⁵ Figure 5(b) presents measurements for Au clusters that have already attained the asymptotic value for the neutralization probability for 1 keV Li^+ ions of 10%.

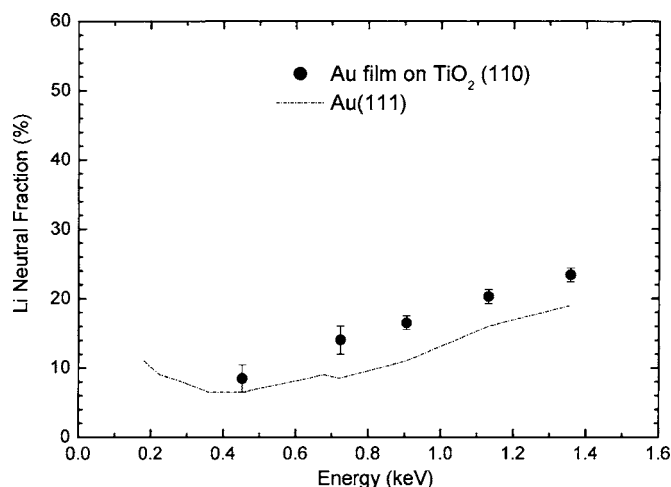


FIG. 6. Energy dependence of the Li neutral fraction for a thick Au film on TiO₂(110) compared with the results of a bulk Au(111) single crystal (from Ref. 36).

These larger clusters presumably have a mean diameter greater than 6 nm (Ref. 15). Comparing the energy dependences shown in Figs. 5(a) and 5(b), we see that the overall behavior of the neutralization probability is similar for Au clusters with different sizes. Nevertheless, smaller Au clusters present a higher neutral fraction, as if the whole curve was shifted up.

As in the case of Ag, we investigated the case of a thick Au film. To achieve the metallization of the substrate, a higher deposition rate was used (1 eq ML/min). Complete coverage of the surface was obtained, as verified by He and Li backscatterings. At the end of the deposition a clear metallic round spot is seen. The Li⁺ neutralization probability measured for this thick Au film is shown in Fig. 6. As may be seen the results for the film are similar to the ones obtained for the large clusters [high coverage in Fig. 5(b)].

The order of the deposited Au film was investigated by LEED and diffuse (111) spots were observed. It is interesting to note here that it had been suggested by Cosandey *et al.*,⁴⁸ who used electron backscattered diffraction (EBSD) in combination with high resolution scanning electron microscopy (HRSEM) to determine the orientation of Au on TiO₂, that Au microcrystals grow on TiO₂(110) in a (111) orientation. Similarly Akita *et al.*⁴⁹ have carried out high resolution transmission electron microscopy (HRTEM) observation of the Au deposition on TiO₂ (anatase and rutile). They observed a preferred orientation relationships between the Au particles and the TiO₂ support, finding that the Au(111) plane is parallel to the TiO₂(110) plane in the case of the rutile support.

A study of Li neutralization on Au(111) was therefore subsequently performed and results similar to the gold film in magnitude were obtained with an increase of the neutral fraction at low energies as for the clusters.³⁶

IV. DISCUSSION

In the previous sections we saw that a higher neutralization fraction is obtained for small clusters at the initial stages of Ag or Au deposition, except at the very beginning, where there is some indication that the neutral fraction would tend

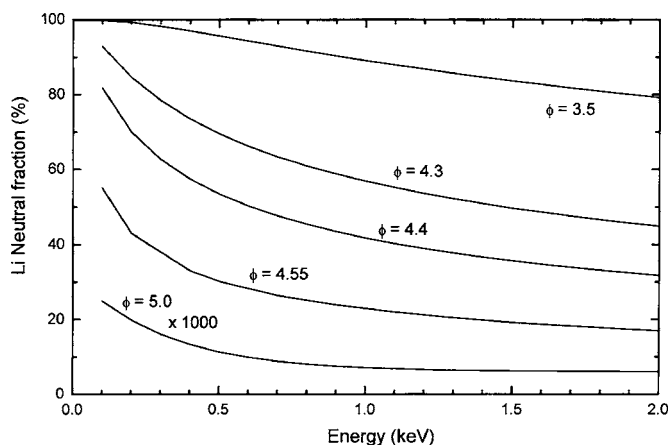


FIG. 7. Calculated Li neutral fraction for a free-electron metal as a function of the beam exit energy for different values of the surface work function. The ion leaves the surface in the normal direction.

to decrease. For larger clusters and in general as the coverage increased, accompanied by growth of cluster size, a smaller neutralization probability was found, which tends to the bulk limit for Ag(111) and Au(111). The energy dependence of the neutralization probability measured for the medium and larger clusters displayed the same trends as for the bulk crystal, although for Au clusters a higher neutralization probability was found for intermediate coverages (cluster sizes).

At present it is difficult to account conclusively for our observations. Indeed a number of factors have to be considered, not all of which are known. In the following we shall try to discuss various facets of this problem, which involves issues such as the work function, morphology, charge, and electronic structure of the supported metal clusters. Electron transfer phenomena in ion/atom-surface interactions (involving bulk solids) have been diversely described depending upon the electronic structure of the surface and type of material (metal/dielectric). In the present case, where one spans material properties from atomic dimension to those of bulk solids rather different descriptions may apply ranging from those appropriate for atom-molecule to atom-solid interaction. We shall briefly delineate these aspects and provide appropriate references to papers presenting a more complete description of these approaches.

Let us first briefly consider the predictions of the free electron model for neutralization of Li, which has been frequently used in the description of interaction with metal surfaces (see, e.g., Ref. 35). In this model one considers electron capture/loss processes depending upon the position of the Li level with respect to the occupied/unoccupied states in the metal, i.e., its position with respect to the Fermi level position. This is determined as a function of the atom-surface distance by the image potential shift. Here we assume a Li ion recedes from the surface and can capture electrons once it is shifted below the Fermi level. Neutralization thus depends on the surface work function.

Figure 7 summarizes the expected values of the Li neutralization fraction within this framework. It displays the energetic dependence of the neutral fraction for different values of the surface work function, calculated for a jellium surface, and assuming that the Li ion leaves the surface along the

surface normal direction. As expected, the neutralization fraction increases for decreasing values of the work function. The energy trend shows the usual dependence on the perpendicular velocity: slower projectiles are more efficiently neutralized since charge transfer will mainly occur in region where capture is favoured. Note here that if we were to consider a Li atom leaving the surface then we would obviously observe an increase in the neutral fraction because of larger survival.

For the case of an ion *leaving* the surface and a surface work function of 4.55 eV, as e.g., the Ag(111), a neutral fraction of 24% is obtained for an exit energy of 835 eV (corresponding to an incident 1 keV beam). In the case of gold, and considering a polycrystalline sample, which has a lower work function ($\varphi=5.1$ eV) than any of the low-index gold single crystal faces [for Au(111), $\varphi=5.4$ eV], the expected value for the neutral Li fraction would be 0.01%. This is due to the fact that the Li(2s) level crosses below the Fermi level of gold for distances of the order of 15–20 a.u. leading to very efficient ionization.

The simplest way in which one could try to rationalize the observation of a larger neutralization probability²¹ on the smaller clusters would be to assume that they are anionic and have a significantly lower work function, which would agree with the measurements of the clusters' electron affinities reported in the gas phase by Taylor *et al.*⁵⁰ Unfortunately we do not have direct measurement of this quantity since our measurements of the work function variation represent an *averaged* work function, which progressively evolves from the TiO₂ value (4.8 eV) to that of the metal: decreasing to about 4.5 eV for Ag and increasing to about 5.3 eV for Au (see also Ref. 21). A conclusive measurement would require a scanning Kelvin probe measurement.

In the case of Ag one could insist that the work function of the small clusters is smaller than 4.55 eV, even if this is not observable, but it seems difficult to explain an *increase* of the average work function for the Au case assuming a smaller work function for one of the surface components. Thus, while the local *cluster* work function certainly has to be considered and should be determined in future experiments, such a simplistic description would not seem reasonable. In the case of gold, two other factors appear in striking disagreement with the jellium model description. The first concerns the energy dependence, which does not correspond to either of the types (decreasing or increasing) mentioned above, though this could be accounted for *assuming* capture on the incoming and outgoing paths. The other most striking feature is the enormous difference between the predictions of the jellium model for surfaces with work functions larger than 5 eV and the results for both the Au clusters, the Au film and the Au(111) single-crystal surface. As may be seen in Fig. 7, one would expect neutral fractions much less than about 0.01% rather than our observed values greater than 10%!

It has been suggested by Liu *et al.*²¹ that cluster charging may play a role. Indeed calculations for very small clusters of few atoms would indicate some charging of the order of

one electron per cluster, but it would seem unlikely that for the larger clusters of few hundred atoms this should be significant.⁵¹

Another aspect of the problem concerns surface roughness and the possible existence of a large number of defect sites at which neutralization could be large. The effect of surface roughness was therefore studied for the Au(111) single crystal. A flat and reconstructed Au(111) surface was prepared by sputtering with 1 keV Ar⁺ and annealing to 800 K in vacuum. The surface was then roughened by 1 keV Ar⁺ ion bombardment for 30 min. The Li⁺ neutralization fraction measured on the rough surface turned out to be lower than the neutral fraction on the annealed Au(111) surface being about 7% rather than 10% at 1 keV.

These observations lead us to the conclusion that the enhancement of the neutralization probability for the small noble metal clusters should be related to specific characteristics of their electronic structure. Before considering this question we are, however, first confronted with the “simpler” question of the anomalous magnitude of the Li⁺ neutralization on the Au(111) surface of the bulk crystal and this brings us to the important problem of a realistic description of the electronic structure of metal surfaces and their effect on neutralization processes. As mentioned earlier in the introduction the (111) surfaces of noble metals are characterized by the existence of projected band gap along the surface normal and the existence of the Shockley surface states. These characteristics of the (111) surfaces can lead to significant alterations of the resonant charge transfer, as known from previous studies^{39,41,52,53} and discussed by us also for band gap and surface states of Ag(100).³⁵ The presence of the bandgap and surface states would lead to strong changes in the position and widths of the Li levels and smaller electron tunnelling rates between the metal and the Li level, leading to larger survival of the occupied Li(2s) level near the surface. A possible explanation³⁶ of some of the characteristics of the Li⁺ neutralization on Au(111) that we observe, could be due to dynamic capture from the partially occupied surface states and the existence of the band gap. Here we would have to consider capture and loss processes on the incoming and outgoing trajectories to account for Au(111) neutral fraction behaviour. It is interesting to note that in a recent study³⁶ of Li⁺ neutralization on Cu(111) (work function of 5.0 eV), in similar scattering conditions, we found results analogous to those for Au(111): a large neutral fraction of the order of 20% at 1 keV and a similar energy dependence. Thus Li neutralization on the noble metals follows trends which appear related to the trends in their electronic structure (see, e.g., Ref. 43). The Ag(111)-type film would appear to give results “not too far” to what may be expected in the jellium model, but for other cases very strong differences exist. Other treatments, such as the many-body treatments of Marston *et al.*,¹⁷ used for the description of alkali scattering on Cu(100) give results somewhat different from the jellium model, but these differences remain relatively small and it does not seem plausible that they would account for the several orders of magnitude we observe. A theoretical investigation of this problem that is currently being undertaken⁵⁴ should allow a better understanding of the processes involved.

Let us now return to the question of clusters. We concluded above that enhancement of the neutralization probability for the small noble metal clusters should be related to specific characteristics of their electronic structure. Without detailed knowledge of the electronic structure of the supported metal clusters of wide size range, we can only suggest possible mechanisms to explain the measured neutral fraction. Previous work has indicated that confined states are present in small noble metal clusters, and that confinement also exists in rather large clusters of about 15 000 atoms.¹¹ We will briefly mention some important experimental results that aimed to determine the electronic structure of supported metal clusters. Very often the metal clusters were grown on different support, but evidence was found of the existence of (111) facets on the top of the clusters. The principal modifications found in the electronic structure of the clusters, when compared to the bulk crystal are outlined below.

- A shift of the 2D surface state band to lower binding energies compared with the onset of the surface state band on macroscopic Au(111) surface was observed by Hövel and Barke¹¹ in an STS and UPS study of Au clusters of about 10⁴ atoms and 2–4 nm height, supported on graphite. This shift depends on the cluster height and can be related to the similar shift observed in thin metal films due to the interaction with the substrate within the decay length of the surface state.⁵⁵
- For gold clusters larger than 10⁴ atoms, Barke and Hövel¹⁰ found a two-dimensional confinement of the Shockley surface states on the (111) facets of the clusters. The quantized levels are located inside the projected bandgap, above the onset of the surface state band. They are created by lateral constraint imposed on the electron's motion by the finite area of the facet.
- For smaller clusters, Barke and Hövel¹¹ found a three-dimensional confinement of the electrons inside the cluster volume. These authors suggested that the surface state disappears below critical cluster size of about 10⁴ atoms.
- Resonances observed in the STS spectra of silver clusters supported on alumina were interpreted by Nilius *et al.*¹² as discretization of the electronic states along the cluster height, similar to the quantum well states (QWS). The QWS were first observed in thin metal films due to the confinement of the conduction electrons perpendicular to the film thickness, which basically corresponds to the one-dimensional particle-in-a-box problem.⁵⁶ The barrier for the electron transmission into the substrate occurs, e.g., for energies within the band gap of the substrate material. Applying the bulk band structure to an Au(111) film, QWS in the occupied region are expected only for energies below the valence band maximum at –1 eV, due to the gap in the surface-projected band structure.
- STM/STS measurements of Valden *et al.*¹³ on Au clusters on TiO₂ show a metal-to-nonmetal transition for clusters smaller than 4 nm and a broadening of the band

gap with decreasing cluster size. Their study of CO oxidation indicated maximum turnover frequency for clusters of the order of 3 nm and a decrease for smaller clusters.

The discussion of neutralization on clusters has clearly to be subdivided into different regions corresponding to specific characteristics of clusters of few atoms to larger clusters whose properties slowly evolve to bulklike characteristics.

The similarities observed between the energy-dependent neutralization fraction on the Au clusters and the Au(111) single-crystal surface would lead us to the conclusion that above a certain size (corresponding to region above about 0.4 eq ML in Fig. 4), our clusters also present several features common to the bulk band structure. We noted above that the Li neutralization increases significantly when one goes from Au(111) to Cu(111), for which the work function is slightly smaller and there is a change in the position of the *L* band gap and surface state that lies closer in resonance with the Li level (see Ref. 43). It is possible that the higher neutralization fractions on the larger clusters are attributable to somewhat similar modification of their electronic structure, i.e., a variation in position of the band gap and surface state of the “metallic” cluster as a function of size would induce changes in neutralization.

For lower cluster sizes further modifications in the clusters' electronic structure mentioned above, such as induction of new states above the surface-state band, as e.g., the appearance of the quantized surface states described by Barke and Hövel¹⁰ may play a significant role. These states are partially populated, since they appear at energies below and above the Fermi level and would certainly affect capture and loss processes. Other types of quantized levels, as e.g., those due to electron confinement in volume, would play significant role in the larger neutralization observed for the smallest clusters.

If our comparisons of the coverage conditions for Au evaporation at evaporation rates similar to those of Lai *et al.*¹⁵ are correct, then neutralization would appear to be most efficient for small cluster sizes of the order of 3 nm, corresponding to the metal-to-nonmetal transition and appearance of a band gap of a few tenths of an electron volt.

The description of neutralization in case of discrete states would obviously have to be different from that of metallic states. In case of *discrete states* non resonant velocity dependent charge transfer processes may play a role as for dielectric surfaces^{57,58} and should be treated using a *molecular description* as this has been done also for ionic solids (see, e.g., Refs. 58 and 59 for details). Electron losses to discrete states (lowest unoccupied molecular orbital (LUMO) and higher) as opposed to the case of the conduction band could be expected to be different and may result in significantly lower losses leading to higher neutralization. One could also expect that the efficiency of electron capture and loss would depend sensitively upon the relative positions of the atomic (here Li) states and the highest occupied molecular orbital (HOMO)/LUMO levels in the cluster. For decreasing cluster sizes transfer of a more strongly bound electron in the HOMO (corresponding to a wider band gap)

could be less efficient leading to a decrease in neutralization efficiency because of increasing “resonance defect” (the extreme case in this evolution would be a metal atom with its fairly high ionization potential). A discussion in terms of a negatively charged cluster,²¹ would have to take into consideration mutual neutralization and the binding energy of an extra electron on the cluster anion.

V. CONCLUSION

In this paper, we presented a detailed study of Li^+ neutralization on Ag and Au clusters supported on TiO_2 . We show that a significantly higher neutralization is observed on small clusters, with possibly a decrease for the smallest clusters. The latter effect is reminiscent of the decrease in catalytic activity observed for very small clusters.^{13,22} These results thus closely follow the size effects observed in the reactivity of these systems mentioned in the introduction.

The energy dependence of the neutralization was studied for the larger clusters (>4 nm) and observed to be somewhat similar in trend to the one observed on films and bulk (111) crystals. For the largest clusters, formed at very low deposition rates, we did not observe any significant changes as a function of coverage, in the studied coverage range, which could be indicative of differences related to 2D and 3D structures.

A general discussion of possible reasons of the enhancement in neutralization is presented and these changes are then tentatively discussed in terms of progressive modifications in the electronic structure of clusters as a function of reduction in size and as it evolves from metallic like to discretised states. The highest neutralization efficiency would appear to correspond to cluster sizes for which a metal-to-nonmetal transition occurs. The relative position of the Li level and the HOMO can be expected to strongly affect the electron transfer processes, which in this case should be described in a molecular framework.

The development of theory of neutralization on the fcc (111) bulk crystals and its extension to the nanoclusters is essential and we hope this work will serve to stimulate this development. A significant progress in these experiments would be the coupling of an STM/STS study of cluster deposition followed by *in situ* neutralization measurements. A valuable contribution would come from experiments with mass selected cluster deposition as in recent elegant experiments of, e.g., Lee *et al.*⁴ Furthermore some experiments on gas-phase interactions of Li^+ with Ag/Au clusters could also be useful, although in this case the role of the interaction with the support would be absent. Our experiments are now being extended to supports other than TiO_2 .

ACKNOWLEDGMENTS

The authors are grateful for various comments on this subject to H.-J. Freund, G.F. Pacchioni, J. Yarmoff, A.G. Borisov, J.P. Gauyacq, and V. Sidis. The authors are also grateful to Yu. Bandurin for help in some experiments.

¹C. R. Henry, Surf. Sci. Rep. **31**, 235 (1998).

²H.-J. Freund, Surf. Sci. **500**, 271 (2002).

³S. Lee, C. Fan, T. Wu, and S. L. Anderson, Surf. Sci. **578**, 5 (2005).

⁴S. Lee, C. Fan, T. Wu, and S. L. Anderson, J. Chem. Phys. **123**, 124710 (2005).

⁵C. T. Campbell, Surf. Sci. Rep. **27**, 1 (1997).

⁶R. L. Johnston, *Atomic and Molecular Clusters* (Taylor & Francis, London, 2002).

⁷B. F. G. Johnson, *Transition Metal Clusters* (Wiley, New York, 1980).

⁸S. A. Nepijko, M. Klimenkov, M. Adelt, H. Kühlenbeck, R. Schlogl, and H.-J. Freund, Langmuir **15**, 5309 (1999).

⁹S.-T. Lee, G. Apai, and M. G. Mason, Phys. Rev. B **23**, 505 (1981).

¹⁰I. Barke and H. Hövel, Phys. Rev. Lett. **90**, 166801 (2003).

¹¹H. Hövel and I. Barke, New J. Phys. **5**, 31 (2003).

¹²N. Nilius, M. Kulawik, H.-P. Rust, and H.-J. Freund, Surf. Sci. **572**, 347 (2004).

¹³M. Valden, X. Lai, and D. W. Goodman, Science **281**, 1647 (1998).

¹⁴T. V. Choudhary and D. W. Goodman, Top. Catal. **21**, 25 (2002).

¹⁵X. Lai, T. P. St. Clair, M. Valden, and D. W. Goodman, Prog. Surf. Sci. **59**, 25 (1998).

¹⁶V. A. Esaulov, Isr. J. Chem. **45**, 13 (2005); H. Winter, Phys. Rep. **367**, 387 (2002).

¹⁷J. B. Marston, D. R. Andersson, E. R. Behringer, B. H. Cooper, C. A. DiRubio, G. Kimmel, and C. Richardson, Phys. Rev. B **48**, 7809 (1993).

¹⁸J. P. Gauyacq and A. G. Borisov, J. Phys.: Condens. Matter **10**, 6585 (1998).

¹⁹A. G. Borisov and J. P. Gauyacq, Surf. Sci. **445**, 430 (2000).

²⁰E. Yu. Usman, I. F. Urazgil'din, A. G. Borisov, and J. P. Gauyacq, Phys. Rev. B **64**, 205405 (2001).

²¹G. F. Liu, Z. Sroubek, and J. A. Yarmoff, Phys. Rev. Lett. **92**, 216801 (2004).

²²M. Haruta, N. Yamada, T. Kobayashi, and S. Iijima, J. Catal. **115**, 301 (1989).

²³M. Haruta, Catal. Today **36**, 153 (1997).

²⁴G. C. Bond and D. T. Thompson, Gold Bull. **33**, 41 (2000).

²⁵M. Haruta, Gold Bull. **37**, 27 (2004).

²⁶S. Cheng and A. Clearfield, J. Catal. **94**, 455 (1985).

²⁷V. I. Bukhtiyarov, A. I. Boronin, and V. I. Savchenko, J. Catal. **150**, 262 (1994).

²⁸A. L. Oliveira, A. Wolf, and F. Schüth, Catal. Lett. **73**, 157 (2001).

²⁹G. R. Bamwenda, S. Tsubota, T. Nakamura, and M. Haruta, Catal. Lett. **44**, 83 (1997).

³⁰X. Lai and D. W. Goodman, J. Mol. Catal. A: Chem. **162**, 33 (2000).

³¹U. Diebold, Surf. Sci. **578**, 1 (2005).

³²A. R. Canário, E. A. Sanchez, Yu. Bandurin, and V. A. Esaulov, Surf. Sci. **547**, L887 (2003).

³³X. Lai, T. P. St. Clair, and D. W. Goodman, Faraday Discuss. **114**, 279 (1999).

³⁴K. Luo, T. P. St. Clair, X. Lai, and D. W. Goodman, J. Phys. Chem. B **104**, 3050 (2000).

³⁵A. R. Canário, A. G. Borisov, J. P. Gauyacq, and V. A. Esaulov, Phys. Rev. B **71**, 121401 (2005).

³⁶A. R. Canário, T. Kravchuk, and V. A. Esaulov, Phys. Rev. (submitted).

³⁷A. G. Borisov, D. Teillet-Billy, J. P. Gauyacq, H. Winter, and G. Dierkes, Phys. Rev. B **54**, 17166 (1996).

³⁸V. A. Ermoshin and A. K. Kazansky, Phys. Lett. A **218**, 99 (1996).

³⁹L. Guillemot and V. A. Esaulov, Phys. Rev. Lett. **82**, 4552 (1999).

⁴⁰A. G. Borisov, A. K. Kazansky, and J. P. Gauyacq, Phys. Rev. Lett. **80**, 1996 (1998).

⁴¹A. G. Borisov, A. K. Kazansky, and J. P. Gauyacq, Phys. Rev. B **59**, 10935 (1999).

⁴²D. Martin, F. Creuzet, J. Jupille, Y. Borensztein, and P. Gadenne, Surf. Sci. **377–379**, 958 (1997).

⁴³E. V. Chulkov, V. M. Silkin, and P. M. Echenique, Surf. Sci. **437**, 330 (1999).

⁴⁴E. Wahlström, N. Lopez, R. Schaub, P. Thosttrup, A. Rønnau, C. Africh, E. Lægsgaard, J. K. Nørskov, and F. Besenbacher, Phys. Rev. Lett. **90**, 26101 (2003).

⁴⁵L. Zhang, R. Persaud, and T. E. Madey, Phys. Rev. B **56**, 10549 (1997).

⁴⁶L. Zhang, F. Cosandey, R. Persaud, and T. E. Madey, Surf. Sci. **439**, 73 (1999).

⁴⁷S. C. Parker, A. W. Grant, V. A. Bondzie, and C. T. Campbell, Surf. Sci. **441**, 10 (1999).

⁴⁸F. Cosandey, R. Persaud, L. Zhang, and T. E. Madey, Mater. Res. Soc. Symp. Proc. **440**, 383 (1997).

⁴⁹T. Akita, K. Tanaka, S. Tsubota, and M. Haruta, J. Electron Microsc. **49**, 657 (2000).

- ⁵⁰ K. J. Taylor, C. L. Pettiette-Hall, O. Cheshnovsky, and R. E. Smalley, *J. Chem. Phys.* **96**, 3319 (1992).
- ⁵¹ G. Pacchioni, (private communication).
- ⁵² J. P. Gauyacq, A. G. Borisov, G. Raseev, and A. K. Kazansky, *Faraday Discuss.* **117**, 15 (2000).
- ⁵³ T. Hecht, H. Winter, A. G. Borisov, J. P. Gauyacq, and A. K. Kazansky, *Phys. Rev. Lett.* **84**, 2517 (2000).
- ⁵⁴ A. Borisov (private communication).
- ⁵⁵ F. Patthey and W.-D. Schneider, *Phys. Rev. B* **50**, 17560 (1994).
- ⁵⁶ F. Patthey and W.-D. Schneider, *Surf. Sci.* **334**, L715 (1995).
- ⁵⁷ H. Shao, D. C. Langreth, and P. Nordlander, *Phys. Rev. B* **49**, 13948 (1994).
- ⁵⁸ A. G. Borisov and V. A. Esaulov, *J. Phys.: Condens. Matter* **12**, R177 (2000).
- ⁵⁹ S. A. Deutscher, A. G. Borisov, and V. Sidis, *Phys. Rev. A* **59**, 4446 (1999).